PLOS ONE

RESEARCH ARTICLE

Comparison of the Transcriptional Profiles of Melanocytes from Dark and Light Skinned Individuals under Basal Conditions and Following Ultraviolet-B Irradiation

Saioa López[1¤]*, Isabel Smith-Zubiaga[2], Alicia García de Galdeano[3], María Dolores Boyano[3,4], Oscar García[5], Jesús Gardeazábal[6], Conrado Martinez-Cadenas[7], Neskuts Izagirre[1], Concepción de la Rúa[1], Santos Alonso[1]

1 Department of Genetics, Physical Anthropology and Animal Physiology. University of the Basque Country UPV/EHU, Leioa, Bizkaia, Spain, **2** Department of Zoology and Animal Cell Biology, University of the Basque Country UPV/EHU, Leioa, Bizkaia, Spain, **3** Department of Cell Biology and Histology. University of the Basque Country UPV/EHU, Leioa, Bizkaia, Spain, **4** BioCruces Health Research Institute, Cruces University Hospital, Cruces-Barakaldo, Bizkaia, Spain, **5** Forensic Genetics Laboratory, Forensic Science Unit, Ertaintza-Basque Country Police, Erandio, Bizkaia, Spain, **6** Dermatology Service, BioCruces Health Research Institute, Cruces University Hospital, Cruces-Barakaldo, Bizkaia, Spain, **7** Department of Medicine, Jaume I University of Castellón, Castellón, Spain

¤ Current address: University College London Genetics Institute (UGI). University College London, London, United Kingdom
* saioa.lopez@ucl.ac.uk

Citation: López S, Smith-Zubiaga I, García de Galdeano A, Boyano MD, García O, Gardeazábal J, et al. (2015) Comparison of the Transcriptional Profiles of Melanocytes from Dark and Light Skinned Individuals under Basal Conditions and Following Ultraviolet-B Irradiation. PLoS ONE 10(8): e0134911. doi:10.1371/journal.pone.0134911

Editor: Thomas G Hofmann, German Cancer Research Center, GERMANY

Received: June 2, 2015

Accepted: July 16, 2015

Published: August 5, 2015

Data Availability Statement: All microarray data are available from the Gene Expression Omnibus database (Accession Number GSE70280).

Funding: This work was supported by the former Spanish Ministerio de Ciencia e Innovación, project CGL2008-04066/BOS to S.A.; by the Dept. Educación, Universidades e Investigación of the Basque Government, project IT542-10 to C.R.; the University of the Basque Country program UFI11/09; a predoctoral fellowship from the Dept. Educación, Universidades e Investigación of the Basque

Abstract

We analysed the whole-genome transcriptional profile of 6 cell lines of dark melanocytes (DM) and 6 of light melanocytes (LM) at basal conditions and after ultraviolet-B (UVB) radiation at different time points to investigate the mechanisms by which melanocytes protect human skin from the damaging effects of UVB. Further, we assessed the effect of different keratinocyte-conditioned media (KCM+ and KCM-) on melanocytes. Our results suggest that an interaction between ribosomal proteins and the P53 signaling pathway may occur in response to UVB in both DM and LM. We also observed that DM and LM show differentially expressed genes after irradiation, in particular at the first 6h after UVB. These are mainly associated with inflammatory reactions, cell survival or melanoma. Furthermore, the culture with KCM+ compared with KCM- had a noticeable effect on LM. This effect includes the activation of various signaling pathways such as the mTOR pathway, involved in the regulation of cell metabolism, growth, proliferation and survival. Finally, the comparison of the transcriptional profiles between LM and DM under basal conditions, and the application of natural selection tests in human populations allowed us to support the significant evolutionary role of *MIF* and *ATP6V0B* in the pigmentary phenotype.

Government to S.L. (BFI09.248). The funders had no role in study design, data collection and analysis, decision to publish, or preparation of the manuscript.

Competing Interests: The authors have declared that no competing interests exist.

Introduction

Melanocytes are melanin-producing cells that, in addition to hold a major role in the pigmentary phenotype, also play an important part in the protection of the skin against the damaging effects of ultraviolet-B (UVB) radiation, such as erythema, sunburn, development of malignant melanoma or other skin cancers [1–4].

The advent of cDNA microarray technology has allowed a preliminary understanding of the gene interactions and regulatory networks that take place in pigmentary cells in response to UVB [5–7]. One of the first reports using cDNA microarrays in various cell lines of human melanocytes for around 9,000 human genes [5] showed that various genes, mainly related to DNA/RNA synthesis and modification, ribosomal proteins or solute carriers and ionic channels, were modulated 4 hours after a single dose of UVB irradiation (100mJ/cm^2). Later, Yang et al. [6] using a higher density microarray (with probes for approximately 47,000 transcripts), although for a single cell line of melanocytes, analysed the response of melanocytes to UVB. In contrast to Valéry et al. [5], Yang et al. [6] selected a 24-hour time point after UVB irradiation and reported a set of p53-target genes as major agents involved in the UV response.

However, many questions remain unsolved yet. For example, although the damage and the collateral consequences of UVB in the human skin are known to differ among individuals of different geographical origin and skin color [8], the different transcriptional responses that could arise between cultured human melanocytes from dark and light donors (hereinafter DM and LM, respectively) have not been completely elucidated. A recent work [9] performed a genome-wide transcriptome analysis of both DM and LM under basal conditions using RNA-Seq technology and found only 16 genes differentially expressed in the two cell types. However, their results could be somehow limited by the small number of melanocyte lines of each type (2 DM and 2 LM) analysed.

Furthermore, the response of melanocytes to UV radiation is known to be mediated by paracrine factors released by keratinocytes, which modulate the growth rate and dendricity of melanocytes, and which ultimately lead to an increased production of melanin [10–18]. In some cases this has been shown by growing melanocytes with keratinocyte conditioned media (KCM) *in vitro;* however, the procedure by which this medium is obtained varies among studies. Thus, while in some experiments this medium is collected after the irradiation of keratinocytes (hereinafter KCM+) [19–20], in other studies the medium is collected from keratinocytes that have not been previously irradiated (hereinafter KCM-) [10, 21–22]. Given the current lack of a consensus to define how to collect this media, we aimed to analyse the putative different responses that might arise when culturing melanocytes with either KCM- or KCM+.

Therefore, the objective of this work was to achieve a full view of the regulatory mechanisms that melanocytes undergo in response to UVB. Thus, we analyse herein the whole-genome transcriptional profile of dark and light melanocytes under basal conditions and after UVB irradiation at different time points (6, 12 and 24 hours) by means of gene expression microarrays. Further, we also aimed to assess the effect of different keratinocyte-conditioned media on melanocytes at a whole-genome level. With that aim, melanocytes were cultured in medium supplemented with keratinocyte-conditioned medium obtained both from non-irradiated (KCM-) and irradiated keratinocytes (KCM+).

This work outperforms previous studies in many regards: 1) we interrogate a large number of probes in the genome, including genes (28,000) and other non-coding RNAs (7,419), 2) we include both DM and LM and assess their transcriptional differences, 3) importantly, we use a relatively high number of biological replicates (6 cell lines of DM and 6 of LM), which minimises the noise from variability among individuals, 4) we perform a time-series analysis that

detects both early and later stress responses and 5) we cultivate melanocytes with KCM- and KCM+ and assess their distinct influence.

Materials and Methods

Cell cultures

Human epidermal keratinocytes were purchased from Cascade Biologics (Life technologies, Carlsbad, CA, USA). Cells were cultured in EpiLife Medium supplemented with human keratinocyte growth supplement (HKGS). Human epidermal melanocytes were also purchased from Cascade Biologics: six lines isolated from lightly pigmented neonatal foreskin (LM), and six lines from darkly pigmented neonatal foreskin (DM). These melanocytes were cultivated in Medium 254 supplemented with 1% human melanocyte growth supplement (HMGS). All the cell lines were maintained in an incubator under an atmosphere of 5% CO_2 at 37°C. Media were refreshed every two days.

UV irradiation and Keratinocyte-conditioned medium

UV irradiation was performed in an ICH2 photoreactor (LuzChem, Canada) at 37°C. Cultures were irradiated at 75 mJ/cm^2 UVB, based on our previous work [20], as we observed that this dosage led to a notable physiological effect but did not affect cell viability in both keratinocytes and melanocytes. Keratinocyte supernatants were harvested from both non-irradiated (KCM-) and irradiated keratinocytes (24 hours after treatment) (KCM+) and kept frozen at -80°C until subsequent use. Subconfluent melanocyte cultures were cultivated in Medium 254 supplemented with HMGS and KCM+ or KCM- medium in a proportion 1:1. The following day they were irradiated with 75 mJ/cm^2 of UVB, and harvested at 6, 12 and 24 hours post irradiation. We used non-irradiated control cultures that were covered by aluminium foil during irradiation (Fig 1).

Microarrays

RNA from irradiated and non-irradiated melanocytes was extracted using the RNA extraction kit from Ambion (Life technologies). Samples were quantified using a UV/VIS NanoDrop 8000 (Thermo Fisher, Waltham, MA, USA), and RNA integrity was analysed through an Agilent 2100 Bioanalyzer using Agilent RNA 6000 Nano Chips (Agilent Technologies, Santa Clara, CA, USA). For each labeling reaction 100 ng RNA were used, with the Low input Quick Amp Labeling kit, one color (Agilent Technologies). First, total RNA was retrotranscribed using AffinityScript Reverse Transcriptase (Agilent Technologies) and Oligo dT primers linked to promoter T7. The synthesized double stranded cDNA was *in vitro* transcribed by T7 RNA polymerase with Cy3-CTP in order to achieve labeled and amplified cRNA. These samples were purified with RNeasy Mini kit columns (Qiagen, Hilden, Germany) and quantified to determinate the yield (which should be higher than 0.825 μg per reaction) and the specific activity of the fluorochrome Cyanine 3 (which should be higher than 6 pmol/μg). All the samples satisfied these requirements. Samples were analysed using SurePrint G3 Human GE Microarrays (Agilent Technologies), which have probes for 27,958 annotated genes and 7,419 long intergenic non-coding RNAs (lincRNAs). The hybridization step was performed using the SureHyb hybridization chamber (Agilent Technologies) and 600 ng of labeled cRNA samples, for 17 hours at 65°C and 10,000 rpms in a hybridization oven. Microarrays were stabilized with ozone-barrier slide covers (Agilent Technologies).

Image processing of the microarrays was performed by using the Agilent Feature Extraction software v10.7.3.1. This software performs 9 evaluation parameters to check the quality of the

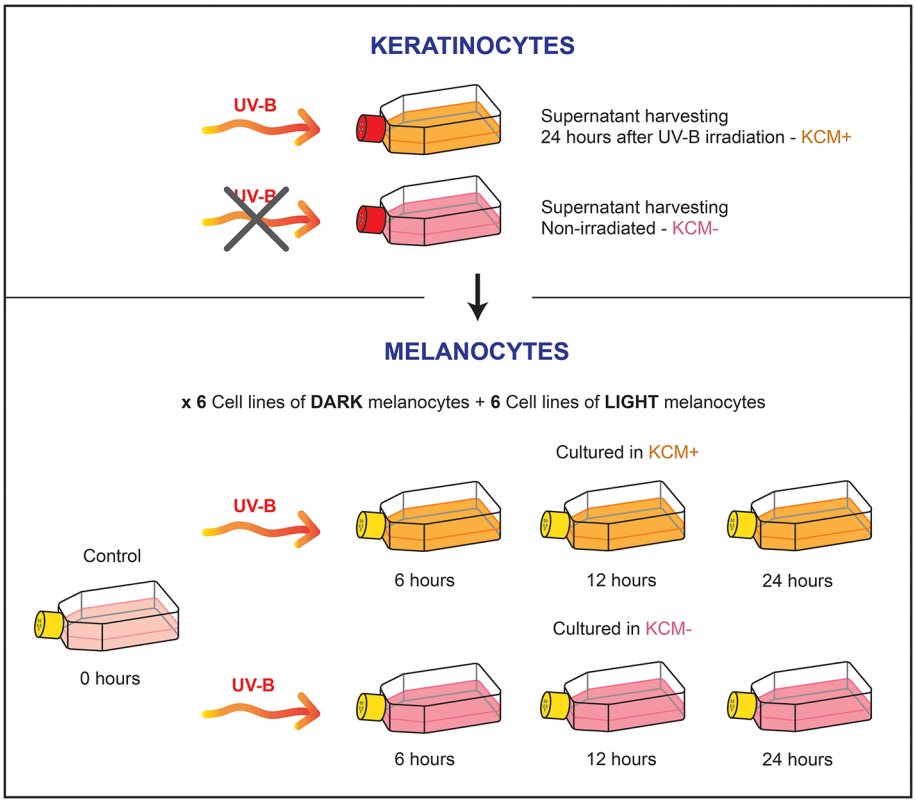

Fig 1. Graphical scheme of the experimental design.

doi:10.1371/journal.pone.0134911.g001

microarrays. The quality control parameters included, among others, the coefficient of variation of the processed signal from non-control probes and spike-ins (%CV), the percentage of outlier probes as regards the replicated probes population, the intensity of the signal of the negative controls and the limit of detection and linearity of the Spike-Ins signal.

Microarray data pre-processing and normalization

Raw data were processed with GeneSpring GX software v11.5.1 (Agilent Technologies). Feature extraction flags were transformed as follows: if feature was not positive and significant, not uniform, not well above background or was a population outlier: compromised; if feature was saturated: not detected.

We performed a variance-stabilizing transformation of the data, which is a key step, but often not considered, in the pre-processing of microarrays data. Most of the subsequent statistical analyses assume that the data follow a normal distribution, with a constant variance independent of the mean of the data. Gene-expression microarray data, however, often have a variance that changes non-linearly with the mean, and thus, log transformations, which are used in the transformation of these data, can inflate the variance of observations near the background. Thus, our data were subjected to a DDHF (Data-Driven Haar-Fisz) transformation for variance stabilization with the R package DDHFm [23]. This method stabilizes the variance of replicated intensities from microarray data and produces transformed intensities that are much closer to the Gaussian distribution than other methods. Furthermore, it can be adapted to different or uncertain distributions, and therefore, it is ideal for the variance stabilization of microarray data.

Data were transformed to log base 2 and normalized following the quantile method [24]. Flag spot information in data files was used to filter probe sets. Entities in which more than 50% of samples in 1 out of any 7 conditions (0h, 6h KCM-, 12h KCM-, 24h KCM, 6h KCM+, 12h KCM+ and 24h KCM+) had "detected" flags were maintained for the analyses.

Quality (QC) Metrics and Principal Component Analysis (PCA)

QC-Metrics was performed with GeneSpring GX software. Gene expression of the transformed and normalized data were subjected to unsupervised classification by means of Principal Component Analysis (PCA) as a preliminary exploratory approach to detect outliers, or the existence of defined clusters based on time points, pigmentation of the cells or the type of KCM used for culture. We used The Unscrambler X v10.3 (CAMO A/S, Trondheim, Norway) and applied the full cross validation method to estimate the stability and performance of the model.

Comparison of expression profiles

Statistical analysis for the comparison of expression profiles was performed with SAM (Significance Analysis of Microarrays, [25]), using two class non-pairwise comparisons and 500 permutations in each test. The significance of the tests was given by the lowest False Discovery Rate at which the gene is called significant based on [26], adjusted for multiple tests.

Pathway enrichment analysis

Enrichment analysis was performed using Web-based Gene Set Analysis Toolkit (WebGestalt) (http://bioinfo.vanderbilt.edu/-webgestalt/option.php), using all the probes analyzed in the microarray as the reference list, and The Kyoto Encyclopedia of Genes and Genomes (KEGG) database of pathways. The significance analysis was performed using the Hypergeometric test. P-values were corrected for multiple tests following the Bonferroni procedure. The minimum number of genes for enrichment was set at 5, and the significance level at Bonferroni adjusted-$p<0.01$, in order to be conservative, avoid false positives and achieve more robust results.

Validation by RT-qPCR

We selected 6 genes showing a change in expression between dark and light melanocytes or after UV irradiation in the microarrays for validation with Real-Time quantitative PCR (RT-qPCR). cDNA was synthesized from 2 μg of total extracted RNA using the First Strand cDNA Synthesis Kit (ThermoFisher) and was used as a template for RT-qPCR analyses. Four different cell lines were analysed (2 of dark melanocytes, and 2 of light melanocytes). RT-qPCR reactions were performed with SYBR Green in a StepOne thermocycler (Life Technologies). Primer sequences (5'-3') were the following: MIFf_GAAGGCCATGAGCTGGTCT, MIFr_GGTTCCT CTCCGAGCTCAC, FDXRf_CTGAGGCAGAGTCGAGTGAAG, FDXRr_CCCGAAGCTCC TTAATGGTGA, TP53I3f_AATGCTTTCACGGAGCAAATTC, TP53I3r_TTCGGTCAC TGGGTAGATTCT, ATP6VOBf_CCATCGGAACTACCATGCAGG, ATP6VOBr_TCCACA GAAGAGGTTAGACAGG, MDM2f_GAATCATCGGACTCAGGTACATC, MDM2r_TCTG TCTCACTAATTGCTCTCCT, RPL6f_ATTCCCGATCTGCCATGTATTC and RPL6r_TAC CGCCGTTCTTGTCACC. Thermocycling conditions were optimized for each pair of primers to obtain 95–100% efficiency and $r^2>0.99$ in the reaction. Gene expression was normalized to the housekeeping gene *GAPDH*. Each reaction was performed in triplicate and values were averaged to calculate relative expression levels.

Selection tests

Preliminary screenings to detect deviations from neutrality were performed using the 1000 Genomes Selection Browser (http://hsb.upf.edu/) [27], which implements several neutrality tests (Tajima's D, Fay & Wu's H, Fu's F, Fu and Li's F*, Fu and Li's D* and EHH, among many others) and provides genome based rank "p-values", that help to identify which SNPs or regions have significantly high scores compared to the rest of the genome.

Further selection tests in candidate loci were performed with DnaSP [28]. We obtained the genotypes of the European (n = 760 chromosomes), African (n = 492) and Asian (n = 572) populations from the 1000 Genomes Project (Phase I May 2011) using SPSmart v5.1.1 (dbSNP build 132) [29]. The orthologous sequence of the chimpanzee was obtained from the UCSC Genome Browser and aligned to the human sequences with ClustalW. For each population, we calculated Tajima's D, Fu & Li's D and Fay & Wu's H with DnaSP [28]. P-values for these tests were obtained using the interface for standard coalescent simulations conditioned on the number of segregating sites.

Results and Discussion

Quality metrics and PCA

QC-Metrics revealed 2 outlier arrays that did not satisfy the quality parameters: L_5.6K- (LM; replicate_5; 6h; KCM-) and L_4.24K- (LM; replicate_4; 24h; KCM-). Thus, those samples were removed from the subsequent statistical analyses.

Second, we performed a Principal Component Analysis (PCA), an exploratory multivariate statistical technique for simplifying complex data sets [30], that has been used for the analysis of microarray data in search of outlier genes [31] or to identify temporal patterns in time-series analyses [32]. The PCA (Fig 2) allowed us to have an overview of the temporal patterns or differentially expressed genes between dark and light melanocytes, or between the culture with KCM+ or KCM-. It showed an apparent general homogeneity, revealing no additional potential outliers and a coherent clustering of our samples according to different variables, which was valuable to discard the presence of outliers or experimental errors. The PCA showed a time-point clustering defined by the second component, revealing a major separation of the samples at 6 hours, while the samples corresponding to 12 and 24 hours clustered close to the controls (0 hours), thus suggesting an early response from melanocytes to UVB that returned again to basal levels after the first 6 hours. At 6 hours we also observed a differential response according to pigmentation defined by the first component. At 24 hours, an apparent clustering regarding the culture of light melanocytes with KCM- or KCM+ was also noticed.

Identification of differentially expressed probes after UVB

A total of 26,493 probes were examined per microarray. By means of SAM [25] we identified the statistically significant differentially expressed genes. Because probes may correspond to both genes and non-coding RNAs, we explicitly indicated when they corresponded to non-coding RNA. We first looked for common genes differentially expressed in DM and LM across time after UVB irradiation. We focused on the top upregulated and downregulated genes at 6, 12 and 24h, and in order to provide robust results, we identified those genes that were significantly up- or downregulated at more than one point (Tables 1 and 2). The adjusted p-value for all these genes was <0.0001.

Common upregulated genes after UVB irradiation. Some of the genes included in this category (Table 1) have already been reported to be associated with the response to ultraviolet irradiation, which gives robustness to our inferences. The most significantly upregulated gene

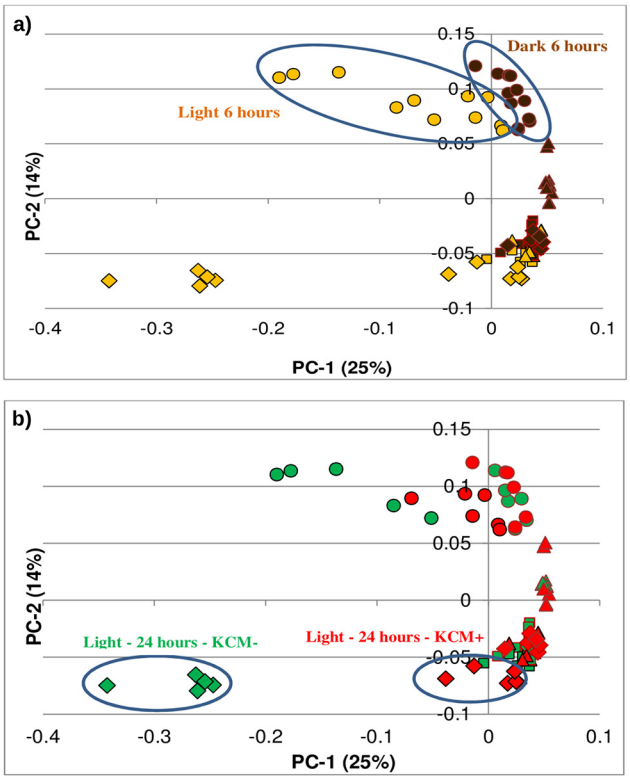

Fig 2. Principal Component Analysis. Charts a) and b) show the same 2-dimesional representation of the data according to the first 2 principal components, but colored according to different variables. Thus, in a) the effects of time (Squares: Time = 0; Dots: Time = 6 hours; Triangles: Time = 12 hours; Diamonds: Time = 24 hours) and pigmentation (Yellow = Light melanocytes; Brown = Dark melanocytes) are highlighted, while in b), it is the time (Squares: Time = 0; Dots: Time = 6 hours; Triangles: Time = 12 hours; Diamonds: Time = 24 hours) and the type of KCM used which are highlighted (Green: KCM-; Red: KCM+).

doi:10.1371/journal.pone.0134911.g002

was *FDXR*, which serves as the first electron transfer protein in all the mitochondrial P450 systems, and has been reported to be upregulated in response to UV irradiation damage in dendritic cells [33] and melanocytes [6]. Importantly, we also observed several genes involved in the regulation of the cell cycle, in the response to stress, in the repair of DNA damage caused by UV that can lead to xeroderma pigmentosum, as well as genes that are associated with melanoma.

We also observed several genes that take part in the regulation of the cell cycle and in the cellular response to stress and that are directly or indirectly involved in the p53 pathway. Some of them modulate P53-mediated apoptosis or cell death in response to stresses like UV irradiation or DNA damage, like *TP53I3*, *PLK3*, *TRIAP1*, *PIDD*, *CDKN1A*, *TP53INP1*, *SESN1*, *BBC3*, *TNFRSF10C*, *DRAM1* and *MDM2*. Other genes that also are upregulated and participate in UV irradiation-induced apoptosis include *RELB* and *EPHA2*.

Another group of the upregulated genes are components of the nucleotide excision repair (NER) pathway that are associated with the reparation of DNA damage caused by UV, and which include *XPC* or *DDB2*. Malfunction of these genes can lead to xeroderma pigmentosum, a recessive disease that is characterized by an increased sensitivity to UV light and a high predisposition for skin cancer development. Several other genes among the top upregulated ones have been reported to be directly or indirectly associated with melanoma, such as *BTG2*, *BAG1*,

Table 1. Most significantly upregulated genes at more than one time point (non-coding RNAs are indicated with *) (Bonferroni-adjusted p-value <0.0001).

Time points	Gene symbol	Accession number	Description
6, 12 and 24h	*FDXR*	NM_004110	ferredoxin reductase, nuclear gene encoding mitochondrial protein
	EPHA2	NM_004431	EPH receptor A2
	RPL6	NM_001024662	ribosomal protein L6
	VWCE	NM_152718	von Willebrand factor C and EGF domains
	UBD	NM_006398	ubiquitin D
	CXCL1	NM_001511	chemokine (C-X-C motif) ligand 1 (melanoma growth stimulating activity, alpha)
	MDM2	NM_002392	Mdm2 p53 binding protein homolog (mouse), transcript variant MDM2
	RPL41	NM_001035267	ribosomal protein L41
	TNFRSF10C	NM_003841	tumor necrosis factor receptor superfamily, member 10c
	DDB2	NM_000107	damage-specific DNA binding protein 2, 48kDa
	GRM2	NM_000839	glutamate receptor, metabotropic 2
	TP53I3	NM_004881	tumor protein p53 inducible protein 3
	ISCU	NM_014301	iron-sulfur cluster scaffold homolog (E. coli)
6 and 12h	*GADD45A*	NM_001924	growth arrest and DNA-damage-inducible, alpha
	PLK3	NM_004073	polo-like kinase 3
	BTG2	NM_006763	BTG family, member 2
	TRIAP1	NM_016399	TP53 regulated inhibitor of apoptosis 1
	PIDD	NM_145886	p53-induced death domain protein
	CDKN1A	NM_078467	cyclin-dependent kinase inhibitor 1A (p21, Cip1)
	TP53INP1	NM_033285	tumor protein p53 inducible nuclear protein 1
	SESN1	THC2527965	Sestrin 1, partial (68%)
	BAG1	NM_004323	BCL2-associated athanogene
	XPC	NM_004628	xeroderma pigmentosum, complementation group C
	*lincRNA chrX:64042150–64093950		
12 and 24h	*RPS2*	NM_002952	ribosomal protein S2
	RPL26	THC2550570	ribosomal protein L26, partial (91%)
	PLXNB2	NM_012401	plexin B2
	KRT17	NM_000422	keratin 17
	ACTA2	NM_001613	actin, alpha 2, smooth muscle, aorta
	SULF2	NM_018837	sulfatase 2
	PVRL4	NM_030916	poliovirus receptor-related 4
	CSRP2	NM_001321	cysteine and glycine-rich protein 2
	DRAM1	NM_018370	DNA-damage regulated autophagy modulator 1
	BBC3	NM_014417	BCL2 binding component 3
	**LOC344887*	NR_033752	NmrA-like family domain containing 1 pseudogene, non-coding RNA
	RELB	NM_006509	v-rel reticuloendotheliosis viral oncogene homolog B
	**LOC642335*	AK098072	cDNA FLJ40753 fis, clone TRACH2001188.
	KIAA1324	NM_020775	KIAA1324
	NOV	NM_002514	nephroblastoma overexpressed gene
	RPS27L	NM_015920	ribosomal protein S27-like
	PRODH	NM_016335	proline dehydrogenase (oxidase) 1, nuclear gene encoding mitochondrial protein
6 and 24h	*GDF15*	NM_004864	growth differentiation factor 15
	NFKBIA	NM_020529	nuclear factor of kappa light polypeptide gene enhancer in B-cells inhibitor, alpha

doi:10.1371/journal.pone.0134911.t001

CXCL1, *PLXNB2*, *CSRP2*, *PRODH* or *GDF15*. Various genes that encode ribosomal proteins such as *RPL6*, *RPL41*, *RPS2*, *RPL26* and *RPS27L* were also observed.

Intriguingly, we observed an upregulation of the gene *NOV*. The protein encoded by this gene is of particular relevance as it has been reported to be essential for the correct development and growth of melanocytes [34]. During development, melanocytes migrate to the epidermis and attach to the basement membrane upon contact with keratinocytes. Development of melanocytes must be tightly regulated and must remain at stable levels in relation to keratinocytes. Fukunaga-Kalabis et al. [34] discovered that *NOV* is upregulated in melanocytes upon contact with keratinocytes in culture, mediating the growth inhibition of melanocytes in order to regulate their spatial location and number. Our results suggest that this gene could also participate in the regulation of melanocytes' growth in response to UVB, most likely by inhibiting their proliferation and allowing either the triggering of cell death or reparation events.

Common downregulated genes after UVB irradiation. Among the top downregulated genes in response to UVB irradiation (Table 2), of particular interest was *LGALS3*, which plays a role in numerous cellular functions including apoptosis, innate immunity, cell adhesion and T-cell regulation, and regulates the expression of several genes that are aberrantly expressed in highly aggressive melanoma cells [**35**]. Another interesting downregulated gene was *PDSS2*, which encodes the prenyl side-chain of coenzyme Q (CoQ), one of the key elements in the respiratory chain. As it has been reported that UV light depletes CoQ10 from the skin [**36**], this consequently suggests that the downregulation of *PDSS2* could be one of the first inducers of reactive oxygen species (ROS) production and, consequently, of oxidative damage to the DNA in the cells ultimately caused by UVB.

Several neuron-related genes were also downregulated by UVB, like ROR1, ERC1, PARD3, SORCS1, LINGO2 and KCNQ2. As neurons and melanocytes share the same embryonic origin (the neural crest) they might likely share some cell regulatory processes [37]. Our results suggest that some genes that are involved in neuronal growth or migration could also be found in melanocytes exerting similar functions. In this regard, it was noticeable that a handful of lincRNAs were also downregulated after UVB irradiation. Although for most lincRNAs biological functions and mechanisms of action remain unknown, our results suggest that some lincRNAs are likely key elements of the regulatory machinery of melanocytes.

Differential transcriptional profile of dark and light melanocytes 6 hours after UVB

As inferred from the unsupervised PCA (Fig 2) the greatest differences among melanocytes were found at 6 hours after UVB irradiation. From that point, melanocytes seem to have started to go back to the basal state. Thus, we focused on determining the differential expression between DM and LM at 6 hours after irradiation (the results for other time points can be found in S1–S4 Tables).

Upregulated genes in LM vs DM 6 hours after UVB irradiation. The significant upregulation of *EDA2R* in LM (Table 3) suggests a putative role for this gene in response to UVB irradiation in light skinned individuals. *EDA2R* has been reported to be affected by recent natural positive selection [**38**–**39**], and its paralog, *EDAR*, has been strongly associated with skin pigmentation variability in humans [**40**]. Strikingly, the intergenic region between *EDA2R* and the next gene on the same chromosome (*AR)* is the most divergent genomic segment between Africans and East Asians in the human genome [**41**].

We also identified as upregulated some genes related to melanoma, like *CDKN2A*, whose expression has already been reported to be induced by UV radiation [42] and which could be conferring light skinned individuals a higher susceptibility to develop melanoma in response to UV radiation, as well as several neuron-related genes and genes associated with the formation

Table 2. Most significantly downregulated genes at more than one time point (non-coding RNAs are indicated with *) (Bonferroni-adjusted p-value <0.0001).

Time points	Gene symbol	Accession number	Description
6, 12 and 24h	*LGALS3*	NM_002306	lectin, galactoside-binding, soluble, 3
	PDSS2	NM_020381	prenyl (decaprenyl) diphosphate synthase, subunit 2
	MAGI3	NM_152900	membrane associated guanylate kinase, WW and PDZ domain containing 3
	PSD3	NM_015310	pleckstrin and Sec7 domain containing 3
	*lincRNA chr10:114583921–114587485 forward strand		
6 and 12h	*SBF2*	NM_030962	SET binding factor 2
	XRCC4	NM_022550	X-ray repair complementing defective repair in Chinese hamster cells 4
	VAV2	NM_003371	vav 2 guanine nucleotide exchange factor
	ROR1	NM_005012	receptor tyrosine kinase-like orphan receptor 1
	ERC1	NM_178040	ELKS/RAB6-interacting/CAST family member 1
	*lincRNA chr17:67547498–67549996 forward strand		
12 and 24h	*HMG20B*	NM_006339	high mobility group 20B
	TUBA1B	NM_006082	tubulin, alpha 1b
	SMYD3	NM_022743	SET and MYND domain containing 3
	SCFD2	NM_152540	sec1 family domain containing 2
	VTI1A	NM_145206	vesicle transport through interaction with t-SNAREs homolog 1A (yeast)
	PRR4	NM_007244	proline rich 4 (lacrimal)
	PARD3	NM_019619	par-3 partitioning defective 3 homolog (C. elegans)
	RABGAP1L	NM_014857	RAB GTPase activating protein 1-like
	TTC28	NM_001145418	tetratricopeptide repeat domain 28
	PCCA	NM_000282	propionyl CoA carboxylase, alpha polypeptide
	MAN1C1	NM_020379	mannosidase, alpha, class 1C, member 1
	A4GALT	NM_017436	alpha 1,4-galactosyltransferase
	MSRA	NM_012331	methionine sulfoxide reductase A
	ANO4	NM_178826	anoctamin 4
	SSBP2	NM_012446	single-stranded DNA binding protein 2
	STX8	NM_004853	syntaxin 8
	REXO1	NM_020695	REX1, RNA exonuclease 1 homolog (S. cerevisiae)
	SH3KBP1	NM_031892	SH3-domain kinase binding protein 1
	BBS9	NM_198428	Bardet-Biedl syndrome 9
	BCKDHB	NM_000056	branched chain keto acid dehydrogenase E1, beta polypeptide
	SORCS1	NM_001206572	sortilin-related VPS10 domain containing receptor 1
	TPK1	NM_022445	thiamin pyrophosphokinase 1
	LINGO2	NM_152570	leucine rich repeat and Ig domain containing 2
	FRY	NM_023037	furry homolog (Drosophila)
	PDE3B	NM_000922	phosphodiesterase 3B, cGMP-inhibited
	KCNQ2	NM_172109	potassium voltage-gated channel, KQT-like subfamily, member 2
	PPIA	THC2525667	Peptidylprolyl isomerase A
	*lincRNA chr2:7214634–7218011 reverse strand		
	*lincRNA chr4:79892901–80229698 forward strand		
	*lincRNA chr18:42263052–42278652 forward strand		
	*lincRNA chr18:74178337–74203637 forward strand		
	*lincRNA chr7:125564239–125734564 forward strand		
6 and 24h	*FAM78B*	NM_001017961	family with sequence similarity 78, member B
	VAV3	NM_006113	vav 3 guanine nucleotide exchange factor

doi:10.1371/journal.pone.0134911.t002

Table 3. Top 50 upregulated genes in LM vs DM at 6 hours after UVB irradiation (non-coding RNAs are indicated with *) (Bonferroni-adjusted p-value <0.0001).

Gene symbol	Accession number	Description
CDKN2A	NM_000077	cyclin-dependent kinase inhibitor 2A (melanoma, p16, inhibits CDK4)
SNAR-A3	NR_024214	small ILF3/NF90-associated RNA A3, small nuclear RNA
KIAA1377	NM_020802	uncharacterized protein KIAA1377
TTC18	NM_145170	tetratricopeptide repeat domain 18
NCAM1	NM_001242607	neural cell adhesion molecule 1, tr. variant 5
HOXB13	NM_006361	homeobox B13
PYCARD	NM_013258	PYD and CARD domain containing
CSRNP3	NM_001172173	cysteine-serine-rich nuclear protein 3
PKMYT1	NM_182687	protein kinase, membrane associated tyrosine/threonine 1
*lincRNA:chr1:85932812–85974062 reverse strand		
QPCT	NM_012413	glutaminyl-peptide cyclotransferase
EDA2R	NM_001242310	ectodysplasin A2 receptor
SGMS1	NM_147156	sphingomyelin synthase 1
RPL37A	NM_000998	ribosomal protein L37a
HIST1H4L	NM_003546	histone cluster 1, H4l
GDPD1	NM_182569	glycerophosphodiester phosphodiesterase domain containing 1
HIST1H3B	NM_003537	histone cluster 1, H3b
*lincRNA:chr10:133738235–133744210 forward strand		
GDPD5	NM_030792	Glycerophosphodiester phosphodiesterase domain containing 5
SUV420H2	NM_032701	suppressor of variegation 4–20 homolog 2 (Drosophila)
MOBKL2B	NM_024761	MOB1, Mps One Binder kinase activator-like 2B (yeast)
MXD3	NM_031300	MAX dimerization protein 3
TUBA1B	NM_006082	tubulin, alpha 1b
SAC3D1	NM_013299	SAC3 domain containing 1
**LOC390595*	NM_001163692	ubiquitin-associated protein 1-like
SNORD15A	NR_000005	small nucleolar RNA, C/D box 15A, small nucleolar RNA
ZNF711	NM_021998	zinc finger protein 711
*lincRNA:chrX:102139220–102156619 forward strand		
LTBP3	ENST00000525443	latent transforming growth factor beta binding protein 3
FAM164A	NM_016010	family with sequence similarity 164, member A
ARHGEF10	ENST00000523711	Rho guanine nucleotide exchange factor (GEF) 10
S100B	NM_006272	S100 calcium binding protein B
HMGN2	NM_005517	high mobility group nucleosomal binding domain 2
C1orf15-NBL1	NM_001204088	C1ORF15-NBL1 readthrough
GALNT14	NM_024572	polypeptide N-acetylgalactosaminyltransferase 14 (GalNAc-T14)
SPTLC3	NM_018327	serine palmitoyltransferase, long chain base subunit 3
IFI27L2	NM_032036	interferon, alpha-inducible protein 27-like 2
RNF6	NM_005977	ring finger protein (C3H2C3 type) 6
TUBB8	NM_177987	tubulin, beta 8
PDGFRL	NM_006207	platelet-derived growth factor receptor-like
ARPC5	ENST00000367534	actin related protein 2/3 complex, subunit 5, 16kDa
PTGDS	NM_000954	prostaglandin D2 synthase 21kDa (brain)
SLC2A13	NM_052885	solute carrier family 2 (facilitated glucose transporter), member 13
CTSF	NM_003793	Cathepsin F
**C1orf133*	NR_024337	SERTAD4 antisense RNA 1
WFDC1	NM_021197	WAP four-disulfide core domain 1

(*Continued*)

Table 3. (*Continued*)

Gene symbol	Accession number	Description
TUBG1	NM_001070	tubulin, gamma 1
SLC12A8	NM_024628	solute carrier family 12, member 8
CXADR	NM_001338	coxsackie virus and adenovirus receptor
SOX5	NM_152989	SRY (sex determining region Y)-box 5

doi:10.1371/journal.pone.0134911.t003

of tubulin, the major constituent of microtubules of the cytoskeleton, and which have been shown to mediate the transport the melanosomes inside the cell [43].

Upregulated genes in DM vs LM 6 hours after UVB irradiation. Next, we focused on the most significant upregulated genes in DM vs LM (Table 4). In this case, we found several genes involved in inflammatory reactions. Some of them have been reported to be particularly involved in sunburn or inflammatory skin reactions in response to UVB, like IL6 [**44**], PTGS2 [**45**] or CCL2 [**46**]. Similarly to LM, DM also showed an upregulation of various genes involved in melanoma progression as well as several genes related to the development of the central nervous system and neuronal processes.

An interesting observation was the upregulation of the *lincRNA MEG3*. The expression of this *lincRNA*, stimulated by cyclic-AMP (cAMP), seems to act as a growth suppressor in tumour cells through the activation of *P53* [47]. As UVR is one of the main stimulatory sources of cAMP, these results suggest that in response to UV radiation, DM upregulate the expression of *MEG3* via cAMP liberation, which could confer protection against melanoma.

Pathway enrichment analysis. Focusing on single loci allows deciphering the differentially expressed genes between different categories (i.e. time or pigmentation). However, although this is useful to determine which genes can be key in the response to UVB, the full biological mechanisms underlying this response may remain obscure. Therefore, we used WebGestalt to look for pathways in KEGG (Kyoto Encyclopedia of Genes and Genomes) that were differentially overrepresented at each time point (Table 5) in LM and DM. We observed that the most significant pathways overrepresented among the upregulated genes corresponded to *ribosome* and *P53 signaling pathway* in both LM and DM. Further analyses using other databases of pathways implemented in WebGestalt (Pathway Commons and Wikipathways) confirmed the involvement of these two pathways in the response to UVB (data not shown).

The role of *P53*, a tumour suppressor that promotes either cell cycle arrest and DNA repair, apoptosis or senescence [48] in the response to UVB has already been reported [6]. Our results are consistent with the proposed mechanism of P53 pathway regulation by ribosomal proteins [49–51]. Thus, we propose that under stress, there is an upregulation of the ribosomal biogenesis leading to an excess of ribosomal proteins that do not participate in the assembly of ribosomes. Instead, these translocate to the nucleoplasm where they interact with MDM2. Under normal conditions, MDM2 binds to the tumour suppressor P53 inhibiting its transcription. But if ribosomal proteins bind to MDM2, then the inhibition of P53 exerted by MDM2 is suppressed. The upregulation of *MDM2* is usually modulated by P53 after the activation of P53-dependent targets, in order to inhibit the activity of P53 and thus restore the normal growth of the cell. However, if the stressing conditions are not completely restablished or DNA damage still exists in the cell, ribosomal proteins could continue interacting with MDM2 to allow to maintain the expression of *P53* (Fig 3). Among the ribosomal proteins that can bind to MDM2 are RPL5 [52] and RPL11 [53], both of which were among the upregulated ribosomal genes in this work.

Table 4. Top 50 upregulated genes in DM vs LM at 6 hours after UVB irradiation (non-coding RNAs are indicated with *) (Bonferroni-adjusted p-value <0.0001).

Gene symbol	Accession numer	Description
HUMRPL26X	THC2550570	ribosomal protein L26 partial (91%)
MMP1	NM_002421	matrix metallopeptidase 1 (interstitial collagenase)
RPL7A	NM_000972	ribosomal protein L7a
CCL2	NM_002982	chemokine (C-C motif) ligand 2
NPTX2	NM_002523	neuronal pentraxin II
COL6A2	NM_058174	collagen, type VI, alpha 2
S100A4	NM_002961	S100 calcium binding protein A4
CXCL1	NM_001511	chemokine (C-X-C motif) ligand 1 (melanoma growth stimulating activity, alpha)
IL6	NM_000600	interleukin 6 (interferon, beta 2)
TMEM158	NM_015444	transmembrane protein 158 (gene/pseudogene)
PAMR1	NM_015430	peptidase domain containing associated with muscle regeneration 1
TMEM8B	NM_001042590	collagen, type VI, alpha 2
CXCL5	NM_002994	chemokine (C-X-C motif) ligand 5
TDRD9	NM_153046	tudor domain containing 9
ANGPTL4	NM_139314	angiopoietin-like 4
PMEPA1	NM_020182	prostate transmembrane protein, androgen induced 1
**MEG3*	NR_003531	maternally expressed 3 (non-protein coding) non-coding RNA
**C1D*	ENST00000412019	C1D nuclear receptor corepressor pseudogene
C1QBP	NM_001212	complement component 1, q subcomponent binding protein
**FAM27A*	NR_024060	family with sequence similarity 27, member A, non-coding RNA
TMEM132A	NM_017870	transmembrane protein 132A
SLC16A2	NM_006517	solute carrier family 16, member 2 (monocarboxylic acid transporter 8)
ANPEP	NM_001150	alanyl (membrane) aminopeptidase
*lincRNA:chr2:239460050–239536125 forward strand		
FN1	NM_054034	fibronectin 1
MYOF	NM_133337	myoferlin
NR4A3	NM_173200	nuclear receptor subfamily 4, group A, member 3
EFS	NM_005864	embryonal Fyn-associated substrate
GRTP1	NM_024719	growth hormone regulated TBC protein 1
TNFRSF11B	NM_002546	tumor necrosis factor receptor superfamily, member 11b
DEF6	NM_022047	differentially expressed in FDCP 6 homolog (mouse)
**FAM27A*	NR_024060	family with sequence similarity 27, member A, non-coding RNA
PTGS2	NM_000963	prostaglandin-endoperoxide synthase 2
GUCA1B	NM_002098	guanylate cyclase activator 1B (retina)
IL1RAP	NM_134470	interleukin 1 receptor accessory protein
SUSD3	NM_145006	sushi domain containing 3
*lincRNA:chr17:73585552–73590170 forward strand		
TNNI3	NM_000363	troponin I type 3 (cardiac)
C10orf116	NM_006829	chromosome 10 open reading frame 116
SPON2	NM_012445	spondin 2, extracellular matrix protein
LYPD1	NM_144586	LY6/PLAUR domain containing 1
IL27RA	NM_004843	interleukin 27 receptor, alpha
FUT1	NM_000148	fucosyltransferase 1 (galactoside 2-alpha-L-fucosyltransferase, H blood group)
CARD9	NM_052813	caspase recruitment domain family, member 9 1
SLC22A17	NM_016609	solute carrier family 22, member 17
IL11	NM_000641	interleukin 11

(*Continued*)

Table 4. (*Continued*)

Gene symbol	Accession numer	Description
TNFAIP2	NM_006291	tumor necrosis factor, alpha-induced protein 2
C15orf48	NM_032413	chromosome 15 open reading frame 48
NT5E	NM_002526	5'-nucleotidase, ecto (CD73)
CXCL3	NM_002090	chemokine (C-X-C motif) ligand 3

doi:10.1371/journal.pone.0134911.t004

On the other hand, several pathways were significantly overrepresented among the genes that were downregulated after UVB exposure, especially in the first 6h in both DM and LM (Table 5). Interestingly, the *adherens junction* pathway was downregulated in both cell types and at different time points. Adherens junctions play an important role maintaining skin homeostasis by mediating the interaction of melanocytes and keratinocytes, which control the proliferation of melanocytes [54], thus preventing the development and progression of melanoma [55].

The effect of keratinocyte conditioned medium

Next, we assessed the expression profiles of melanocytes supplemented with keratinocyte-conditioned medium obtained both from non-irradiated (KCM-) and irradiated keratinocytes (KCM+). Again, differentially expressed genes were obtained with SAM and we performed a pathway enrichment analysis (Table 6). We did not observe any significantly downregulated pathways in melanocytes growing with KCM+ vs KCM-. As regards the upregulated pathways, various pathways were affected in LM, most of them related to *signaling pathways*. We did not detect any upregulated pathway in DM, which suggests that DMs could have lower requirements for keratinocyte-derived factors to start the response mechanisms against UV irradiation. On the contrary, LM show a significant upregulation of several pathways when cultivated with KCM+ compared to KCM-, which could suggest that for these cells, the type or the concentration of factors present in KCM- is not enough and they require more factors to engage in certain metabolic activities.

Among the results obtained, of particular interest was the *mTOR signaling pathway*, which was upregulated in LM at 6h after UVB irradiation growing in KCM+. mTOR can be activated by UVR through the triggering of growth factor receptors bearing receptor tyrosine kinase (RTK) activity [56–58] like keratinocyte-derived EGF, FGF or HGF. mTOR signaling reciprocally interacts with p53 as a life/death regulator of irradiated skin cells. It has been shown that upon activation by UVR, mTOR can inhibit apoptosis and force cell cycle transition, or drive cells into senescence. This work reveals that the keratinocyte-derived factors activate the mTOR signaling pathway in LM to induce cell proliferation, consistent with the upregulation of cell cycle observed later at 24 hours. We propose that in this case mTOR forces cell cycle transition. This, however, could increase the susceptibility to develop melanoma, especially if DNA damage caused by UVB has not been repaired yet. In fact, mTOR pathway has been shown to be activated in the majority of malignant melanomas [59]. The fact that this pathway was activated in LM in culture with KCM+ suggests that some keratinocyte-derived factors, secreted after the irradiation of keratinocytes with UVB, could also be at the base of melanocytes' malignancy.

Other signaling pathways that were upregulated in the presence of KCM+ are also activated by keratinocyte derived factors, such as the neurotrophin signaling pathway, which is activated by NGF and promotes the survival of melanocytes.

Table 5. KEGG pathway enrichment analysis of the upregulated and downregulated genes in DM and LM after UVB irradiation.

	DM		LM	
	Pathway	**Adj-p**	**Pathway**	**Adj-p**
Upregulated at 6h	p53 signaling pathway	9.49E-07	p53 signaling pathway	7.04E-07
	Ribosome	3.00E-04	Ribosome	2.43E-06
Upregulated at 12h	Ribosome	3.22E-11	Systemic lupus erythematosus	1.16E-06
	RNA transport	7.11E-07	Ribosome	1.47E-06
	Ribosome biogenesis in eukaryotes	7.00E-04	p53 signaling pathway	1.10E-03
	p53 signaling pathway	2.13E-02	Mismatch repair	5.40E-03
			Pathways in cancer	6.90E-03
			Apoptosis	7.90E-03
Upregulated at 24h	Ribosome	1.06E-09	Ribosome	7.38E-06
	p53 signaling pathway	1.50E-03		
Downregulated at 6h	Adherens junction	1.51E-08	Ubiquitin mediated proteolysis	6.84E-12
	Ubiquitin mediated proteolysis	7.21E-08	Adherens junction	5.23E-11
	Wnt signaling pathway	9.12E-06	Endocytosis	6.14E-06
	Colorectal cancer	3.53E-05	Wnt signaling pathway	3.14E-05
	Progesterone-mediated oocyte maturation	4.04E-05	Progesterone-mediated oocyte maturation	5.32E-05
	Endocytosis	6.24E-05	Cell cycle	7.36E-05
	Pathways in cancer	7.60E-05	Insulin signaling pathway	5.00E-04
	Systemic lupus erythematosus	1.00E-04	Oocyte meiosis	7.00E-04
	Cell cycle	9.00E-04	Pathways in cancer	7.00E-04
	Oocyte meiosis	1.00E-03	Colorectal cancer	1.20E-03
	Endometrial cancer	1.10E-03	Neurotrophin signaling pathway	2.60E-03
	Fc epsilon RI signaling pathway	1.70E-03	Fc gamma R-mediated phagocytosis	8.60E-03
	B cell receptor signaling pathway	1.80E-03	Endometrial cancer	1.18E-02
	ErbB signaling pathway	1.90E-03	Chronic myeloid leukemia	1.54E-02
	Fc gamma R-mediated phagocytosis	2.20E-03	Bacterial invasion of epithelial cells	1.76E-02
	T cell receptor signaling pathway	2.50E-03	Fc epsilon RI signaling pathway	2.11E-02
	Insulin signaling pathway	5.30E-03	Chemokine signaling pathway	4.22E-02
	Neurotrophin signaling pathway	1.97E-02	ErbB signaling pathway	4.22E-02
			T cell receptor signaling pathway	4.22E-02
Downregulated at 12h	Metabolic pathways	4.43E-05	Protein processing in endoplasmic reticulum	2.00E-03
	Adherens junction	1.00E-04		
	Fc gamma R-mediated phagocytosis	3.00E-04		
	Propanoate metabolism	1.10E-03		
	Protein processing in endoplasmic reticulum	2.70E-03		
	Systemic lupus erythematosus	3.10E-03		
	Purine metabolism	4.90E-03		
	Regulation of actin cytoskeleton	1.20E-02		
	Valine, leucine and isoleucine degradation	4.30E-02		
	Pyrimidine metabolism	4.30E-02		
Downregulated at 24h			Cell cycle	2.20E-08
			Systemic lupus erythematosus	8.56E-06
	-		DNA replication	2.54E-05
			Oocyte meiosis	2.00E-03
			Lysine degradation	2.12E-02

doi:10.1371/journal.pone.0134911.t005

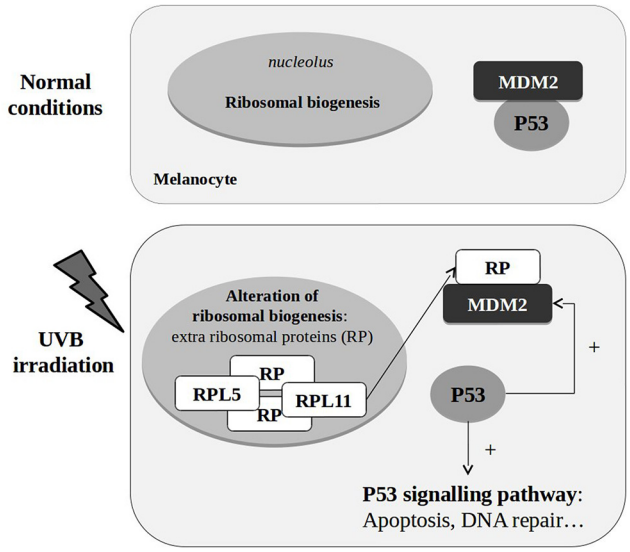

Fig 3. Proposed mechanism for the involvement of ribosomal proteins, MDM2 and p53 signaling pathway in the response to UVB irradiation.

doi:10.1371/journal.pone.0134911.g003

Identification of differentially expressed genes in LM and DM under basal conditions

In order to identify putative candidate genes involved in normal pigmentation variability, we compared the transcriptional profiles of DM and LM under basal conditions (i.e. at time 0, without irradiation). No significantly overrepresented pathways were observed here. Therefore, we focused on the 50 most significant genes in each category (Tables 7 and 8). The most significant genes upregulated in LM (Table 7) were *ATP6V0B* and *ATP6VOD1*. These encode two

Table 6. KEGG pathway enrichment analysis for genes upregulated in the culture with KCM+ vs KCM- (significant pathways for the downregulated ones were not observed).

	LM		DM	
	Pathway	**Adj-p**	**Pathway**	**Adj-p**
6h	Ubiquitin mediated proteolysis	1.00E-03	-	
	mTOR signaling pathway	4.34E-02		
12h	Neurotrophin signaling pathway	8.03E-05	-	
	Phosphatidylinositol signaling system	5.50E-03		
	Endocytosis	2.28E-02		
24h	RNA transport	1.50E-03	Focal adhesion	4.85E-05
	Insulin signaling pathway	4.70E-03		
	Ubiquitin mediated proteolysis	4.90E-03		
	Homologous recombination	7.60E-03		
	mRNA surveillance pathway	8.30E-03		
	SNARE interactions in vesicular transport	9.50E-03		
	Spliceosome	1.24E-02		
	Cell cycle	1.66E-02		
	Pyrimidine metabolism	1.89E-02		
	Ribosome biogenesis in eukaryotes	2.23E-02		
	Wnt signaling pathway	4.46E-02		

doi:10.1371/journal.pone.0134911.t006

Table 7. Top 50 upregulated genes in LM vs DM under basal conditions (non- coding RNAs are indicated with *) (bonferroni-adjusted p-value <0.0001).

Locus name	Accession number	Description
ATP6V0B	NM_004047	ATPase, H+ transporting, lysosomal 21kDa, V0 subunit b
ATP6V0D1	NM_004691	ATPase, H+ transporting, lysosomal 38kDa, V0 subunit d1
FUT6	NM_000150	fucosyltransferase 6 (alpha (1,3) fucosyltransferase)
SLC16A12	NM_213606	solute carrier family 16, member 12
HSCB	NM_172002	HscB iron-sulfur cluster co-chaperone homolog (E. coli)
ZNF865	NM_001195605	zinc finger protein 865
EFS	NM_005864	embryonal Fyn-associated substrate
KRT31	NM_002277	keratin 31
RPL36A-HNRNPH2	NM_001199973	RPL36A-HNRNPH2 readthrough
JMJD5	NM_001145348	jumonji domain containing 5
HIST1H4C	NM_003542	histone cluster 1, H4c
GFRA3	NM_001496	GDNF family receptor alpha 3
KIAA1826	NM_032424	KIAA1826
DNAJC19	NM_145261	DnaJ (Hsp40) homolog, subfamily C, member 19
HAP1	NM_177977	huntingtin-associated protein 1
UXS1	NM_025076	UDP-glucuronate decarboxylase 1
SCAMP1	NM_004866	secretory carrier membrane protein 1
LTA4H	NM_000895	leukotriene A4 hydrolase
DYNC1LI1	NM_016141	dynein, cytoplasmic 1, light intermediate chain 1
LRRFIP2	NM_006309	leucine rich repeat (in FLII) interacting protein 2
C10orf88	NM_024942	chromosome 10 open reading frame 88
PDCD1	NM_005018	programmed cell death 1
MZT2A	ENST00000491265	mitotic spindle organizing protein 2A
MCM3	NM_002388	minichromosome maintenance complex component 3
C6orf163	NM_001010868	chromosome 6 open reading frame 163
DTX4	NM_015177	deltex homolog 4 (Drosophila)
CLCN6	NM_021735	chloride channel 6 (CLCN6)
RFK	NM_018339	riboflavin kinase
WHSC2	NM_005663	Wolf-Hirschhorn syndrome candidate 2
FGFRL1	NM_001004356	fibroblast growth factor receptor-like 1
BTBD6	NM_033271	BTB (POZ) domain containing 6
N4BP1	NM_153029	NEDD4 binding protein 1
MAP2K6	NM_002758	mitogen-activated protein kinase kinase 6
POMP	NM_015932	proteasome maturation protein
GABPA	NM_002040	GA binding protein transcription factor, alpha subunit 60kDa
UPF3A	NM_023011	UPF3 regulator of nonsense transcripts homolog A (yeast)
PLEKHA3	NM_019091	pleckstrin homology domain containing, family A member 3
CD276	NM_001024736	CD276 molecule (CD276)
ENTPD2	NM_203468	ectonucleoside triphosphate diphosphohydrolase 2
DEDD	NM_032998	death effector domain containing
FAM70B	ENST00000375348	family with sequence similarity 70, member B
MCM5	NM_006739	minichromosome maintenance complex component 5
*LOC100131257**	NR_034022	zinc finger protein 655 pseudogene
SCARNA13	NR_003002	small Cajal body-specific RNA 13
SMNDC1	NM_005871	survival motor neuron domain containing 1
CALML4	NM_033429	calmodulin-like 4

(*Continued*)

Table 7. (*Continued*)

Locus name	Accession number	Description
C1orf131	NM_152379	chromosome 1 open reading frame 131
RNGTT	NM_003800	RNA guanylyltransferase and 5'-phosphatase
KCNQ3	NM_004519	potassium voltage-gated channel, KQT-like subfamily, member 3
WASF3	NM_006646	WAS protein family, member 3

doi:10.1371/journal.pone.0134911.t007

components of the V-ATPase, which is responsible for maintaining an adequate acidic environment within melanosomes for the synthesis of melanin [60]. The most significantly upregulated gene in DM compared to LM (Table 8) was *MIF*. *MIF* has been identified as a regulator of melanogenesis, as it shows D-dopachrome tautomerase activity, which transforms D-dopachrome, dopaminechrome or its derivatives into precursors of melanin or neuromelanin [61]. It has also been suggested that *MIF* mediates melanogenesis in the skin through the activation of protease-activated receptor (PAR-2) and stem cell factor (SCF) expression in keratinocytes after exposure to UVB [62]. Interestingly, Polimanty et al [63] reported a correlation between the CNV 22q11.23 containing the gene *MIF* with environmental variables. In particular, they suggested that *MIF*-related gene dosage could be associated with the adaptation to UVR, and that darker skins were correlated with haplotypes carrying no deletions. Copy number variability, and the higher frequency of deletions at this locus in light skinned individuals could be leading to a decreased *MIF* gene dosage, as observed in this work.

For the other genes in Tables 7 and 8 we did not find any evident direct correlation with pigmentary phenotype.

Validation by RT-qPCR

Six genes were selected for validation of the microarrays' results, which showed either a change of expression after UV treatment or a differential expression between LM and DM (*ATP6VOB*, *TP53I3*, *MDM2*, *MIF*, *RPL6* and *FDXR*), and measured their expression levels by quantitative real-time PCR (RT-qPCR). We assessed the expression of 4 melanocytic cell lines (2 DM and 2 LM) at basal conditions and at 6 and 12 hours after UVB irradiation. The expression patterns and direction of changes of all of the genes were consistent with the microarray data (Fig 4), observing a significant increase in the expression of *TP53I3*, *MDM2*, *RPL6* and *FDXR* in both LM and DM after UVB. The expression analysis of *ATP6VOB* and *MIF* also supported the differential expression of these genes by LM and DM, being *ATP6VOB* more expressed by LM, while *MIF* was more significantly expressed by DM (both at basal conditions and after UVB irradiation).

Natural selection tests

In order to assess the biological relevance of the genes that were differentially expressed between DM and LM under basal conditions, we performed evolutionary neutrality tests on these genes (Tables 7 and 8) using the populations from the 1000 Genomes Project (1KGP). For this, we performed a first screening of different neutrality tests using the 1000 Genomes Selection Browser to identify putative signatures of selection. After multiple test correction, the gene *ATP6V0D1* (ATPase, H+ Transporting, Lysosomal 38kDa, V0 Subunit D1) seemed to deviate from neutrality in the European populations.

Further neutrality tests using DnaSP [28] supported significant signatures of selection acting on *ATP6V0D1* in Europeans (Tajima's D: -2.31, p-value = 0; Fay & Wu's H: -10.66, p-value = 0.001), thus suggesting that this gene might be involved in human pigmentary phenotype. This

Table 8. Top 50 upregulated genes in DM vs LM under basal conditions (non- coding RNAs are indicated with *) (bonferroni-adjusted p-value <0.0001).

Locus name	Accession number	Description
MIF	NM_002415	macrophage migration inhibitory factor
*TTC19**	ENST00000395886	tetratricopeptide repeat domain 19
CYTB	ENST00000361789	mitochondrially encoded cytochrome b
NBEA	NM_015678	neurobeachin
CTSO	NM_001334	cathepsin O
SNORA23	NR_002962	small nucleolar RNA, H/ACA box 23
PMP22	NM_000304	peripheral myelin protein 22
CXCL1	NM_001511	chemokine ligand (melanoma growth stimulating activity, alpha)
CDKN2A	NM_058197	cyclin-dependent kinase inhibitor 2A (melanoma, p16)
LDB3	NM_001171610	LIM domain binding 3
MIPEP	NM_005932	mitochondrial intermediate peptidase
MAPK8	NM_139047	mitogen-activated protein kinase 8
SNORD15A	NR_000005	small nucleolar RNA, C/D box 15A
*SNAR-A3**	NR_024214	small ILF3/NF90-associated RNA A3
ASCC1	NM_015947	activating signal cointegrator 1 complex subunit 1
ZNF235	NM_004234	zinc finger protein 235
MBIP	NM_001144891	MAP3K12 binding inhibitory protein 1
C13orf38	NM_001198908	chromosome 13 open reading frame 38
*LOC100132707**	NR_024477	hypothetical LOC100132707
UTRN	NM_007124	utrophin
CALM2	NM_001743	calmodulin 2 (phosphorylase kinase, delta)
*MOCS1**	NM_005943	molybdenum cofactor synthesis 1
ZNF212	NM_012256	zinc finger protein 212
KIAA0090	NM_015047	KIAA0090 (KIAA0090)
SNORD3B-1	NR_003271	small nucleolar RNA, C/D box 3B-1
HLX	NM_021958	H2.0-like homeobox
C9orf72	NM_145005	chromosome 9 open reading frame 72
SEC23B	NM_032985	Sec23 homolog B (S. cerevisiae)
WRAP73	NM_017818	WD repeat containing, antisense to TP73
MAN1A1	NM_005907	mannosidase, alpha, class 1A, member 1
S100B	NM_006272	S100 calcium binding protein B
CCDC93	NM_019044	coiled-coil domain containing 93
ZNF3	NM_032924	zinc finger protein 3
FTH1	NM_002032	ferritin, heavy polypeptide 1
RAB30	NM_014488	RAB30, member RAS oncogene family
RDM1	NM_001034836	RAD52 motif 1
BTAF1	NM_003972	BTAF1 RNA polymerase II,
HLA-F	NM_018950	major histocompatibility complex, class I, F
CABYR	NM_012189	calcium binding tyrosine-(Y)-phosphorylation regulated
MAP4K2	NM_004579	mitogen-activated protein kinase 2
PRPF18	ENST00000320054	PRP18 pre-mRNA processing factor 18 homolog (S. cerevisiae)
CALM3	NM_005184	calmodulin 3 (phosphorylase kinase, delta)
ALKBH4	NM_017621	alkB, alkylation repair homolog 4 (E. coli)
*LOC399744**	NR_024497	hypothetical LOC399744
SETD6	NM_024860	SET domain containing 6
SH3TC2	NM_024577	SH3 domain and tetratricopeptide repeats 2
ARHGAP35	NM_004491	Rho GTPase activating protein 35
CHCHD6	NM_032343	coiled-coil-helix-coiled-coil-helix domain containing 6
RC3H2	NM_018835	ring finger and CCCH-type domains 2
WDR46	NM_005452	WD repeat domain 46

doi:10.1371/journal.pone.0134911.t008

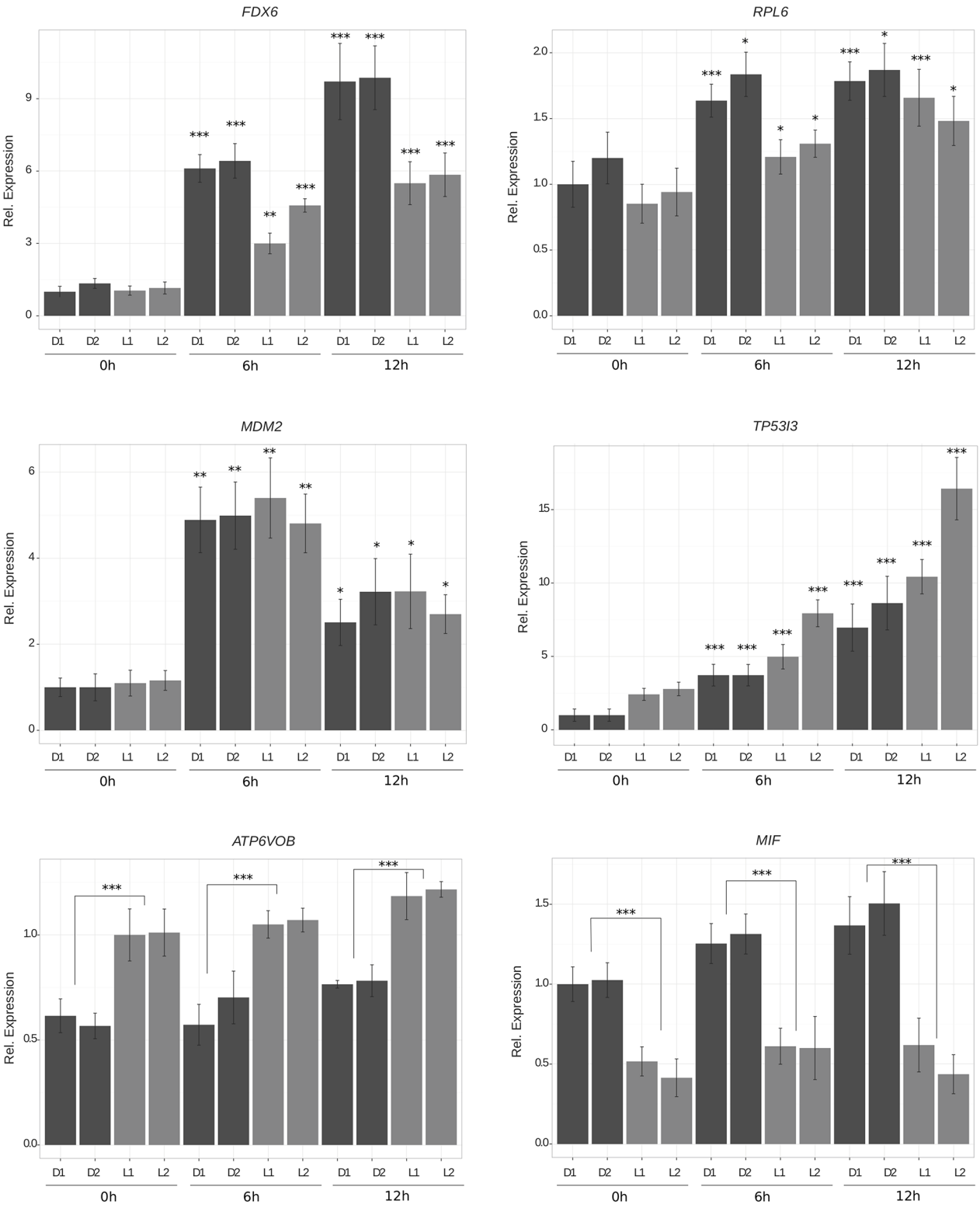

Fig 4. Gene expression of genes *FDX6*, *RPL6*, *MDM2*, *TP53I3*, *ATP6VOB* and *MIF* assessed by RT-qPCR. Unpaired t-test; *** p<0.0001; ** p<0.001; * p<0.01.

doi:10.1371/journal.pone.0134911.g004

reinforces the notion that selective pressures can shape pigmentation variability by driving the evolution of melanosomal genes. So, besides the well-known *OCA2*, *SLC45A2* and *SLC24A5*, we support *ATP6V0D1* as an additional melanosomal-membrane gene that has been subjected to selective pressures and might be involved in pigmentation variability in Europeans.

No deviations from neutrality were detected in any population for the *MIF* gene (data not shown). However, we should take into account that *MIF* is embedded in a CNV [63] and in a previous work we observed how a variation in copy number can interfere with neutrality tests by altering the frequencies of polymorphisms leading to an excess of detected homozygosity [64]. A loss of copies would result in apparent homozygosity, and duplications of one allele would mask possible variant alleles in sequencing or genotyping experiments. Therefore, although with the available tools and our knowledge we cannot detect deviations from neutrality, we cannot still exclude the possibility that this gene is under selection.

Conclusions

We have provided an overview of the most significant genes that are up and downregulated in response to UVB irradiation and revealed the interaction of ribosomal proteins and P53 signaling pathway in the response to UVB in both DM and LM. We have also observed that DM and LM show differentially expressed genes after irradiation and in particular in the first 6 hours. These are mainly associated with inflammatory skin reactions, cell survival or melanoma. Furthermore, the culture with KCM+ compared with KCM- had a noticeable effect on LM, but not in DM, triggering various signaling pathways in LM such as the mTOR signaling pathway. And importantly, the comparison of the transcriptional profile of LM and DM under basal conditions allowed us to highlight the significant involvement of *MIF* and *ATP6V0B* in the normal variability of human skin pigmentation.

Supporting Information

S1 Table. Top 50 upregulated genes in LM vs DM 12 hours after UVB.
(PDF)

S2 Table. Top 50 upregulated genes in DM vs LM 12 hours after UVB.
(PDF)

S3 Table. Top 50 upregulated genes in LM vs DM 24 hours after UVB.
(PDF)

S4 Table. Top 50 upregulated genes in DM vs LM 24 hours after UVB.
(PDF)

Acknowledgments

The authors thank for technical and human support provided by the Genomics and Proteomics Service of the UPV/EHU (SGIker).

Author Contributions

Conceived and designed the experiments: SL ISZ SA. Performed the experiments: SL ISZ AGG SA. Analyzed the data: SL ISZ SA. Contributed reagents/materials/analysis tools: MDB OG JG CMC NI CR AGG. Wrote the paper: SL ISZ SA.

References

1. Young AR. The sunburn cell. Photodermatol. 1987; 4: 127–134. PMID: 3317295
2. Kricker A, Armstrong BK, English DR. Sun exposure and non-melanocytic skin cancer. Cancer Cause Control. 1994; 5: 367–392.
3. Elwood JM. Melanoma and sun exposure. Semin Oncol. 1996; 23: 650–666. PMID: 8970584
4. Povey JE, Darakhshan F, Robertson K, Bisset Y, Mekky M, Rees J, et al. DNA repair gene polymorphisms and genetic predisposition to cutaneous melanoma. Carcinogenesis. 2007; 28: 1087–1093. PMID: 17210993
5. Valéry C, Grob JJ, Verrando P. Identification by cDNA microarray technology of genes modulated by artificial ultraviolet radiation in normal human melanocytes: relation to melanocarcinogenesis. J Invest Dermatol. 2001; 117: 1471–1482. PMID: 11886511
6. Yang G, Zhang G, Pittelkow MR, Ramoni M, Tsao H. Expression profiling of UVB response in melanocytes identifies a set of p53-target genes. J Invest Dermatol. 2006; 126: 2490–2506. PMID: 16888633
7. Alonso S, Izagirre N, Smith-Zubiaga I, Gardeazabal J, Díaz-Ramón JL, Díaz-Pérez JL, et al. Complex signatures of selection for the melanogenic loci TYR, TYRP1 and DCT in humans. BMC Evol Biol. 2008; 8: 74. doi: 10.1186/1471-2148-8-74 PMID: 18312627
8. Tadokoro T, Yamaguchi Y, Batzer J, Coelho SG, Zmudzka BZ, Miller SA, et al. Mechanisms of skin tanning in different racial/ethnic groups in response to ultraviolet radiation. J Invest Dermatol. 2005; 124: 1326–1332. PMID: 15955111
9. Haltaufderhyde KD, Oancea E. Genome-wide transcriptome analysis of human epidermal melanocytes. Genomics. 2014; 104: 482–489. doi: 10.1016/j.ygeno.2014.09.010 PMID: 25451175
10. Gordon PR, Mansur CP, Gilchrest BA. Regulation of human melanocyte growth, dendricity, and melanization by keratinocyte derived factors. J Invest Dermatol. 1989; 92: 565–572. PMID: 2467948
11. Yaar M, Grossman K, Eller M, Gilchrest BA. Evidence for nerve growth factor-mediated paracrine effects in human epidermis. J Cell Biol. 1991; 115: 821–828. PMID: 1655813
12. Chakraborty AK, Funasaka Y, Slominski A, Ermak G, Hwang J, Pawelek JM, et al. Production and release of proopiomelanocortin (POMC) derived peptides by human melanocytes and keratinocytes in culture: regulation by ultraviolet B. Biochim Biophys Acta. 1996; 1313: 130–138. PMID: 8781560
13. Hirobe T. Endothelins are involved in regulating the proliferation and differentiation of mouse epidermal melanocytes in serum-free primary culture. J Invest Dermatol Symp Proc. 2001; 6: 25–31.
14. Hirobe T, Osawa M, Nishikawa S. Steel factor controls the proliferation and differentiation of neonatal mouse epidermal melanocytes in culture. Pigm Cell Res. 2003; 16: 644–655.
15. Hirobe T, Osawa M, Nishikawa S. Hepatocyte growth factor controls the proliferation of cultured epidermal melanoblasts and melanocytes from newborn mice. Pigm Cell Res. 2004; 17: 51–61.
16. Scott G, Leopardi S, Printup S, Malhi N, Seiberg M, Lapoint R. Proteinase-activated receptor-2 stimulates prostaglandin production in keratinocytes: analysis of prostaglan- din receptors on human melanocytes and effects of PGE2 and PGF2a on melanocyte dendricity. J Invest Dermatol. 2004; 122: 1214–1224. PMID: 15140225
17. Yamaguchi Y, Brenner M, Hearing VJ. The regulation of skin pigmentation. J Biol Chem. 2007; 282: 27557–27561. PMID: 17635904
18. Abdel-Malek ZA, Kadekaro AL, Swope VB. Stepping up melanocytes to the challenge of UV exposure. Pigm Cell Melanoma R. 2010; 23: 171–186.
19. Jamal S, Schneider RJ. UV-induction of keratinocyte endothelin-1 downregulates E-cadherin in melanocytes and melanoma cells. J Clin Invest. 2002; 110: 443–452. PMID: 12189238
20. López S, Alonso S, García de Galdeano A, Smith-Zubiaga I. Melanocytes from dark and light skin respond differently after ultraviolet B irradiation: effect of keratinocyte conditioned medium. Photodermatol Photoimmunol Photomed. 2015; 31: 149–158. doi: 10.1111/phpp.12169 PMID: 25740555
21. Abdel-Naser MB. Differential effects on melanocyte growth and melanization of low vs. high calcium keratinocyte-conditioned medium. Br J Dermatol. 1999; 140: 50–55. PMID: 10215767
22. Maeda K, Tomita Y. Mechanism of the Inhibitory Effect of Tranexamic Acid on Melanogenesis in Cultured Human Melanocytes in the Presence of Keratinocyte-conditioned Medium. J Health Sci. 2007; 53: 389–396.
23. Motakis ES, Nason GP, Fryzlewicz P, Rutter GA. Variance stabilization and normalization for one-color microarray data using a data-driven multiscale approach. Bioinformatics. 2006; 22: 2547–2453. PMID: 16877753

24. Bolstad BM, Irizarry RA, Astrand M, Speed TP. A Comparison of Normalization Methods for High Density Oligonucleotide Array Data Based on Bias and Variance. Bioinformatics. 2003; 19: 185–193. PMID: 12538238

25. Tusher VG, Tibshirani R, Chu G. Significance analysis of microarrays applied to the ionizing radiation response. Proc Natl Acad Sci U S A. 2001; 98: 5116–5121. PMID: 11309499

26. Storey JD. A direct approach to false discovery rates. J Roy Stat Soc B. 2002; 64: 479–498.

27. Pybus M, Dall'Olio GM, Luisi P, Uzkudun M, Carreño-Torres A, Pavlidis P, et al. 1000 Genomes Selection Browser 1.0: a genome browser dedicated to signatures of natural selection in modern humans. Nucleic Acids Res. 2014; 42: D903–909. doi: 10.1093/nar/gkt1188 PMID: 24275494

28. Librado P, Rozas J. DnaSP v5: a software for comprehensive analysis of DNA polymorphism data. Bioinformatics. 2009; 25: 1451–1452. doi: 10.1093/bioinformatics/btp187 PMID: 19346325

29. Amigo J, Salas A, Phillips C, Carracedo A. SPSmart: adapting population based SNP genotype databases for fast and comprehensive web access. BMC Bioinformatics. 2008; 9: 428. doi: 10.1186/1471-2105-9-428 PMID: 18847484

30. Basilevsky A. Statistical Factor Analysis and Related Methods, Theory and Applications. John Wiley & Sons. New York; 1994.

31. Hilsenbeck SG, Friedrichs WE, Schiff R, O'Connell P, Hansen RK, Osborne CK, et al. Statistical Analysis of Array Expression Data as Applied to the Problem of Tamoxifen Resistance. J Natl Cancer Institute. 1999; 91: 453–459.

32. Chu S, DeRisi J, Eisen M, Mulholland J, Botstein D, Brown PO, et al. The transcriptional program of sporulation in budding yeast. Science. 1998; 282: 699–705. PMID: 9784122

33. de la Fuente H, Lamana A, Mittelbrunn M, Perez-Gala S, Gonzalez S, García-Diez A, et al. Identification of genes responsive to solar simulated UV radiation in human monocyte-derived dendritic cells. PLoS ONE. 2009; 4: e6735. doi: 10.1371/journal.pone.0006735 PMID: 19707549

34. Fukunaga-Kalabis M, Martinez G, Liu ZJ, Kalabis J, Mrass P, Weninger W, et al. CCN3 controls 3D spatial localization of melanocytes in the human skin through DDR1. J Cell Biol. 2006; 175: 563–569. PMID: 17101694

35. Braeuer RR, Zigler M, Kamiya T, Dobroff AS, Huang L, Choi W, et al. Galectin-3 Contributes to Melanoma Growth and Metastasis via Regulation of NFAT1 and Autotaxin. Cancer Res. 2012; 15: 5757–5766.

36. Baumann L. How to Prevent Photoaging? J Invest Dermatol. 2005; 125: 7–13.

37. Yaar M, Park HY. Melanocytes: a window into the nervous system. J Invest Dermatol. 2012; 132: 835–845. doi: 10.1038/jid.2011.386 PMID: 22158549

38. Sabeti PC, Varilly P, Fry B, Lohmueller J, Hostetter E, Cotsapas C, et al. Genome-wide detection and characterization of positive selection in human populations. Nature. 2007; 18: 913–918.

39. Hilmer AM, Freudenberg J, Myles S, Herms S, Tang K, Hughes DA, et al. Recent positive selection of a human androgen receptor/ectodysplasin A2 receptor haplotype and its relationship to male pattern baldness. Hum Genet. 2009; 126: 255–264. doi: 10.1007/s00439-009-0668-z PMID: 19373488

40. Hider JL, Gittelman RM, Shah T, Edwards M, Rosenbloom A, Akey JM, et al. Exploring signatures of positive selection in pigmentation candidate genes in populations of East Asian ancestry. BMC Evol Biol. 2013; 13: 150. doi: 10.1186/1471-2148-13-150 PMID: 23848512

41. Casto AM, Henn BM, Kidd JM, Bustamante CD, Feldman MW. A tale of two haplotypes: the EDA2R/AR Intergenic region is the most divergent genomic segment between Africans and East Asians in the human genome. Hum Biol. 2012; 84: 641–694. PMID: 23959643

42. Parvey S, Conroy S, Russell T, Gabrielly B. Ultraviolet radiation induces p16 expression in human skin. Cancer Res. 1999; 59: 4185–4189. PMID: 10485451

43. Rogers SL, Karcher RL, Roland JT, Minin AA, Steffen W, Gelfand VI. Regulation of melanosome movement in the cell cycle by reversible association with myosin V. J Cell Biol. 1999; 146: 1265–1276. PMID: 10491390

44. Urbanski A, Schwarz T, Neuner P, Krutmann J, Kimbauer R, Köck A, et al. Ultraviolet light induces increased circulating interleukin-6 in humans. J Invest Dermatol. 1990; 94: 808–811. PMID: 2355183

45. Buckman SY, Gresham A, Hale P, Hruza G, Anast J, Masferrer J, et al. COX-2 expression is induced by UVB exposure in human skin: implications for the development of skin cancer. Carcinogenesis. 1998; 19: 723–729. PMID: 9635856

46. Purwar R, Wittmann M, Zwirner J, Oppermann M, Kracht M, Dittrich-Breiholz O, et al. Induction of C3 and CCL2 by C3a in keratinocytes: a novel autocrine amplification loop of inflammatory skin reactions. J Immunol. 2006; 177: 4444–4450. PMID: 16982879

47. Zhou Y, Zhong Y, Wang Y, Zhang X, Batista DL, Gejman R, et al. Activation of p53 by MEG3 non-coding RNA. J Biol Chem. 2007; 282: 24731–24742. PMID: 17569660

48. Rufini A, Tucci P, Celardo I, Melino G. Senescence and aging: the critical roles of p53. Oncogene. 2013; 32: 5129–5143. doi: 10.1038/onc.2012.640 PMID: 23416979

49. Zhang Y, Lu H. Signaling to p53: ribosomal proteins find their way. Cancer Cell. 2009; 16: 369–377. doi: 10.1016/j.ccr.2009.09.024 PMID: 19878869

50. Deisenroth C, Zhang Y. Ribosome biogenesis surveillance: probing the ribosomal protein-Mdm2-p53 pathway. Oncogene. 2010; 29: 4253–4260. doi: 10.1038/onc.2010.189 PMID: 20498634

51. Donati G, Montanaro L, Derenzini M. Ribosome biogenesis and control of cell proliferation: p53 is not alone. Cancer Res. 2012; 72: 1602–1607. doi: 10.1158/0008-5472.CAN-11-3992 PMID: 22282659

52. Dai MS, Lu H. Inhibition of MDM2-mediated p53 ubiquitination and degradation by ribosomal protein L5. J Biol Chem. 2004; 279: 44475–44482. PMID: 15308643

53. Lohrum MA, Ludwig RL, Kubbutat MH, Hanlon M, Vousden KH. Regulation of HDM2 activity by the ribosomal protein L11. Cancer Cell. 2003; 3: 577–587. PMID: 12842086

54. Garrod DR. Desmosomes and hemidesmosomes. Curr Opin Cell Biol. 1993; 5: 30–40. PMID: 8448028

55. Haass NK, Herlyn M. Normal human melanocyte homeostasis as a paradigm for understanding melanoma. J Investig Dermatol Symp Pro. 2005; 10: 153–163.

56. Jean C, Hernandez-Pigeon H, Blanc A, Charveron M, Laurent G. Epidermal growth factor receptor pathway mitigates UVA-induced G2/M arrest in keratinocyte cells. J Invest Dermatol. 2007; 127: 2418–2424. PMID: 17495959

57. Cao C, Lu S, Kivlin R, Wallin B, Card E, Bagdasarian A, et al. AMP-activated protein kinase contributes to UV- and H2O2-induced apoptosis in human skin keratinocytes. J Biol Chem. 2008; 283: 28897–28908. doi: 10.1074/jbc.M804144200 PMID: 18715874

58. He YY, Council SE, Feng L, Chignell CF. UVA-induced cell cycle progression is mediated by a disintegrin and metalloprotease/epidermal growth factor receptor/AKT/Cyclin D1 pathways in keratinocytes. Cancer Res. 2008; 68: 3752–3758. doi: 10.1158/0008-5472.CAN-07-6138 PMID: 18483258

59. Karbowniczek M, Spittle CS, Morrison T, Wu H, Henske EP. mTOR is activated in the majority of malignant melanomas. J Invest Dermatol. 2008; 128: 980–987. PMID: 17914450

60. Dooley CM, Schwarz H, Mueller K, Mongera A, Konantz M, Neuhauss SC, et al. Slc45a2 and V-ATPase are regulators of melanosomal pH homeostasis in zebrafish, providing a mechanism for human pigment evolution and disease. Pigment Cell Melanoma Res. 2013; 26: 205–217. doi: 10.1111/pcmr.12053 PMID: 23205854

61. Matsunaga J, Sinha D, Solano F, Santis C, Wistow G, Hearing V. Macrophage migration inhibitory factor (MIF)—its role in catecholamine metabolism. Cell Mol Biol. 1999; 45: 1035–1040. PMID: 10644007

62. Enomoto A, Yoshihisa Y, Yamakoshi T, Ur Rehman M, Norisugi O, Hara H, et al. UV-B radiation induces macrophage micgration inhibitory factor-mediated melanogenesis through activation of protease-activated receptor-2 and stem cell factor in keratinocytes. Am J Pathol. 2011; 178: 679–687. doi: 10.1016/j.ajpath.2010.10.021 PMID: 21281800

63. Polimanti R, Piacentini S, Iorio A, De Angelis F, Kozlov A, Novelletto A, et al. Haplotype differences for copy number variants in the 22q11.23 region among human populations: a pigmentation-based model for selective pressure. Eur J Hum Genet. 2015; 23: 116–123. doi: 10.1038/ejhg.2014.47 PMID: 24667780

64. López S, García I, Smith I, Sevilla A, Izagirre N, de la Rúa C, et al. Discovery of Copy Number Variants by Multiplex Amplifiable Probe Hybridization (MAPH) in candidate pigmentation genes. Ann Hum Biol. 2014; 24: 1–9.